

In Operando Micro-Raman Three-Dimensional Thermometry with Diffraction-Limit Spatial Resolution for GaN-based Light-Emitting Diodes

T. Park,¹ Yong-Jing Guan,^{1,2} Zhi-Qiang Liu,³ and Yong Zhang^{1,*}

¹Department of Electrical and Computer Engineering, University of North Carolina at Charlotte, Charlotte, North Carolina 28223, USA

²Guangxi Key Laboratory for Relativistic Astrophysics, School of Physical Science and Technology, Guangxi University, Nanning 530004, China

³Institute of Semiconductors, Chinese Academy of Science, Beijing 100086, China

(Received 23 February 2018; revised manuscript received 1 July 2018; published 24 September 2018)

Confocal micro-Raman microscopy performed in the transparent spectral region of a semiconductor can, in principle, be used for *operando* three-dimensional (3D) thermometry with optical diffraction-limit spatial resolution. However, when applied to high-power GaN-based light-emitting diodes (LEDs), the applicability is hindered by the often strong secondary electroluminescence in the visible spectral region that overwhelms the Raman signal. We develop a “split-time-window” scheme that can mimic the continuous wave operation but without the interference of the secondary emission, which allows us to carry out noninvasive 3D temperature profiling and comprehensive thermal analyses of the whole device at any operation current. The technique is applied to an $(In_xGa_{1-x})N/GaN$ LED to extract its 3D temperature distribution when operated at 350 mA with μm -scale resolution when using a 532-nm laser. We show that although a conventional technique can yield a reliable average temperature difference between the heat sink and the LED junction (a few degrees), the spatial fluctuations are much larger than the average difference. Furthermore, we show that using the anti-Stokes to Stokes Raman intensity ratio as a metric can yield more reliable and accurate results than using the Raman frequency shift.

DOI: 10.1103/PhysRevApplied.10.034049

I. INTRODUCTION

Due to its direct and wide band gap and chemical stability, gallium nitride (GaN) is an attractive material for microelectronic and optoelectronic applications, such as display and general lighting and power electronics [1–4]. However, it is well known that the efficiency of the GaN-based light-emitting diodes (LEDs) tends to decrease with increasing temperature and/or injection current, a phenomenon known as efficiency droop. Although the mechanisms of the droop remain inconclusive, high-injection current-induced heating is thought to be a contributing factor [5]. The well-known current-crowding effect is expected to induce inhomogeneity in temperature [6]. Heating and inhomogeneous temperature distribution under a high operational current are also significant for the power electronic device [7]. Therefore, a reliable method to evaluate the temperature distribution of GaN-based devices under real operational conditions with both high spatial resolution and accuracy is important for improving the device performance. Diverse measurement methods have been adopted to quantify the junction temperature

of GaN and other LEDs, including a forward-voltage method [8], thermal resistance and thermal transient methods [9], electroluminescence (EL) peak shift [10], photoluminescence (PL) peak shift [11], micro-Raman frequency shift [12–14], and infrared (IR) thermography [15]. These methods typically measure the average temperature of LEDs as a whole [8–11], but sometimes they also measure the two-dimensional surface temperature distribution [12–15]. However, it is known that the device temperature is nonuniform both laterally and vertically under operation [13]. A micro-Raman-based method using a visible laser can, in principle, provide noninvasive *operando* 3D thermometry but with better spatial resolution than IR thermography. Unfortunately, yellow luminescence [16], typically ranging from 440 to 700 nm, originating from deep-level defects in GaN, often overwhelms the Raman scattering signal under the operating conditions of GaN LEDs. Only to some extent, for instance under a relatively low injection current, can the luminescence interference be mitigated by using a long-wavelength laser [12]. Additionally, using the Raman frequency shift [12–14] as a temperature calibration could be problematic, because temperature change also leads to stress relaxation that also contributes to the Raman frequency shift [17,18].

*yong.zhang@uncc.edu

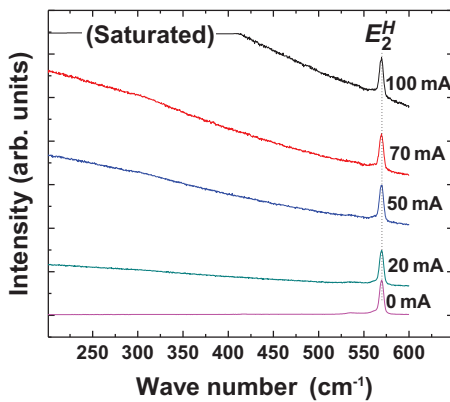


FIG. 1. PL/Raman spectra at different currents of $I = 0, 20, 50, 70, 100$ mA.

In this study, we develop a confocal micro-Raman based 3D temperature imaging technique that can not only achieve diffraction-limit spatial resolution (approximately $1 \mu\text{m}$) and high accuracy (approximately $\pm 2^\circ\text{C}$), but also suppress all EL interference when applied to GaN-based LEDs using any below-band-gap laser. We use the intensity ratio of anti-Stokes and Stokes Raman scattering lines, instead of the shift of the Stokes line, to extract the temperature, which is immune to the interference of heating-induced stress relaxation.

II. EXPERIMENT

The $(\text{In}_x\text{Ga}_{1-x})\text{N}/\text{GaN}$ LED is grown on a c -plane patterned sapphire substrate by using metal organic chemical vapor deposition. Five-pairs of $(\text{In}_x\text{Ga}_{1-x})\text{N}/\text{GaN}$ multiple quantum wells (MQWs) with 2.5-nm wells and 12-nm barrier thicknesses are used as the active layer having a peak emission wavelength of 448 nm. The fabrication details can be found in a previous publication [19]. The device size is $1.15 \times 1.15 \text{ mm}^2$. The LED chip is mounted on a ceramic heat sink without phosphor. The Stokes and anti-Stokes GaN Raman signals are measured in air using a confocal Raman microscope (Horiba LabRAM HR800 with a 1200 g mm^{-1} grating) with a 532-nm laser and a notch filter. The laser power used is 22.8 mW with a $\times 50$ long-working-distance (LWD) objective lens. It is found that the relatively high laser power induced some residual heating effects, which led to an increase in sample temperature by $2.7 \pm 0.5^\circ\text{C}$. We have subtracted this amount from the measured temperature. Because of the presence of the relatively strong yellow emission [16], even at a moderate injection current level the Raman signals become unresolvable, as shown in Fig. 1 where PL/Raman spectra at $I = 0, 20, 50, 70$, and 100 mA are measured in a conventional way. Therefore, a more versatile method is needed to eliminate the yellow emission and still be able to mimic realistically the high-current operational conditions.

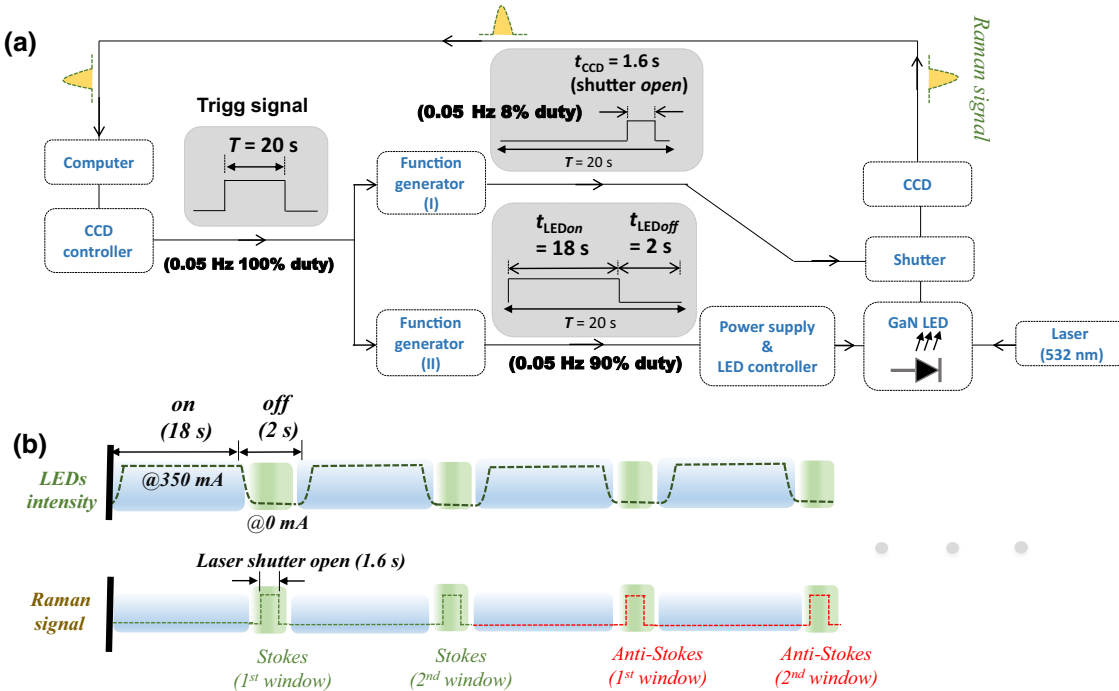


FIG. 2. Schematic diagrams and timing sequences for measuring Raman signals without the interference of EL signal when an $(\text{In}_x\text{Ga}_{1-x})\text{N}/\text{GaN}$ LED is operated at high current. (a) Block diagrams of the measurement technique, (b) timing sequences of a LED in operation and off operation for Raman measurement (in the case illustrated, Stokes and anti-Stokes signals are measured in two spectral windows, twice for each window).

The general idea of our approach is to drive LEDs under a continuous current for a relatively long period of time to allow the device to reach a steady operational state, then switch the power off briefly to take the Raman spectrum in the middle of the off-time window. This approach resembles the “stress-probe” measurement used for electronic devices [20]. We take advantage of the fact that the electronic relaxation time is much faster than the thermal relaxation time so that the luminescence decays quickly after the device is turned off but the thermal distribution remains nearly the same as in a truly continuous mode during the Raman data collection window. The implementation of this “split-time-window” method is shown schematically in Fig. 2 with block diagrams and timing sequences. The charge-coupled-device (CCD) controller of the Raman microscope is set to have an apparent data collection time T and outputs a transistor-transistor-logic (TTL) signal with an on-time of T (e.g., $T=20$ s). This

signal is split to drive two function generators (FG-I and FG-II; AFG310, Tektronix) simultaneously: FG-I outputs a square function that is used to control a LED controller (RC120, Gradasoft Vision Ltd.) such that the LED is on and off during t_{LEDon} and $t_{LEDooff}$, respectively, with $t_{LEDon} + t_{LEDooff} = T$ (e.g., $t_{LEDon} = 18$ s and $t_{LEDooff} = 2$ s). FG-II outputs a square function at the center of $t_{LEDooff}$ for a time interval t_{CCD} to open a mechanical shutter in front of the CCD. The t_{CCD} is the actual signal collection time such that $t_{LEDooff} = t_{CCD} + 2\delta t$ (δt is a buffer of 0.2 s) to avoid the possible overlapping between the luminescence and Raman signals (e.g., $t_{CCD} = 1.6$ s). The measurement can be repeated multiple times for one spectral window to achieve an adequate signal-to-noise ratio and cover multiple spectral windows as needed, with the assurance that the timing is always correct. In this study, two spectral windows are used to cover the Stokes and anti-Stokes Raman lines.

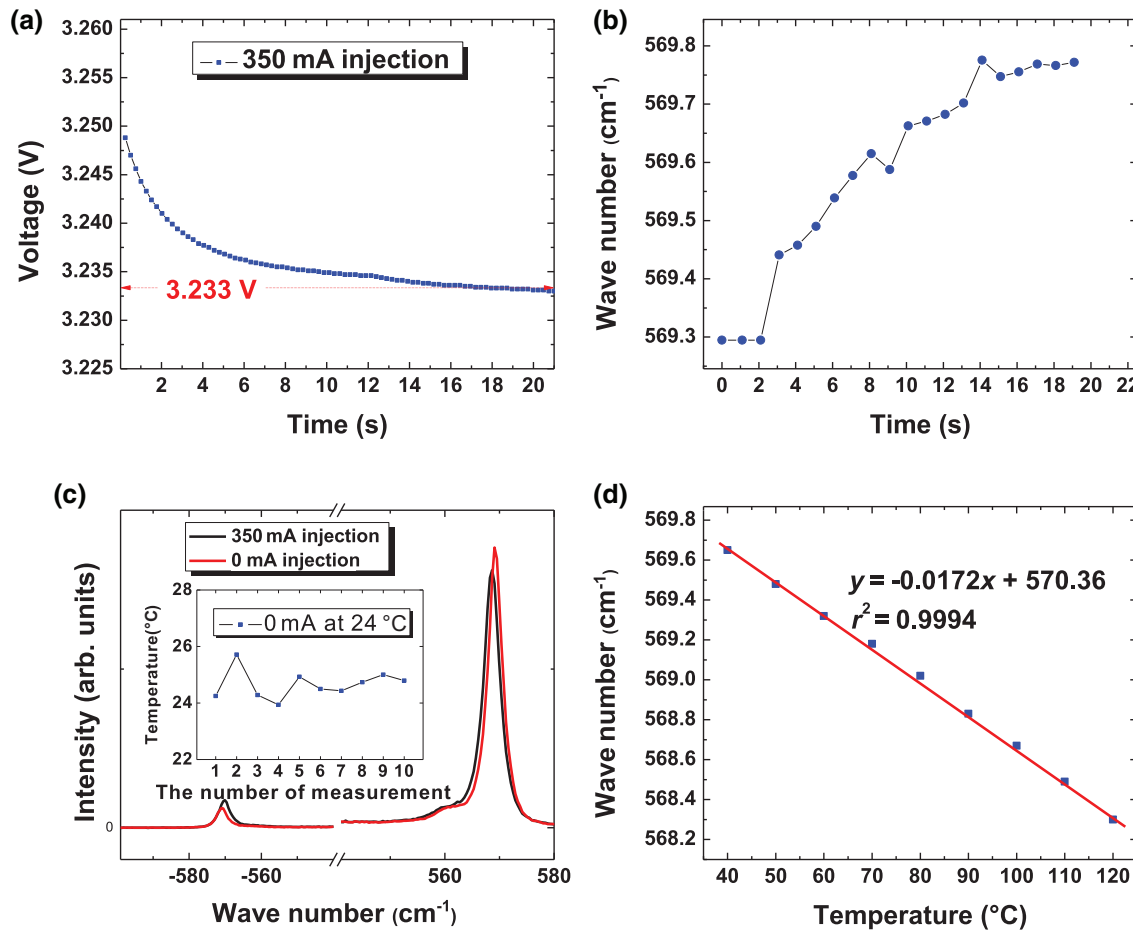


FIG. 3. Characterization of an $(In_xGa_{1-x})N/GaN$ LED. (a) Time-dependent voltage at a 350-mA injection current. (b) Time dependence of GaN E_2^H mode frequency at 350 mA. (c) Stokes and anti-Stokes Raman scattering signals of GaN E_2^H mode at 350 mA with the EL yellow emission suppressed compared with zero current. Inset shows the temperatures of 10 repeated measurements from a single location. (d) Temperature dependence of GaN E_2^H mode frequency at zero current.

III. RESULTS AND DISCUSSION

Here we illustrate how to determine the appropriate measurement parameters under a 350-mA injection current. It is well known that the diode forward voltage can be used indirectly to estimate the junction temperature of GaN LEDs [8]. In this method, at a constant current injection the junction temperature will not be equilibrated until the forward voltage is stabilized. As shown in Fig. 3(a), at a 350-mA current injection, the forward voltage approaches about 3.233 V after 14 s, indicating that the junction temperature will not change much further after 14 s. It has been reported that the junction temperature of GaN LEDs stabilized after 10 s under a 350-mA injection [21]. To be safe, we adopted $t_{LEDon} = 18$ s. Typically, the GaN E_2^H phonon of approximately 570 cm⁻¹ is employed to monitor the temperature change of GaN LEDs [12–14,22]. To determine a time interval in which the device temperature exhibits minimal change after being turned off, we measure time-dependent Raman in a time duration of 20 s right after the t_{LEDon} on-period, with the time dependence of the E_2^H mode frequency shown in Fig. 3(b). It changes from 569.24 to 569.76 cm⁻¹ but there is no change within the first 2 s, which suggests that the device temperature is maintained during the initial 2 s. Thus, we select $t_{CCD} = 1.6$ s for each spectral window and $t_{LEDoff} = 2$ s. As shown in Fig. 3(c), the sharp peaks of Stokes and anti-Stokes Raman scattering are measured successfully without any interference from the yellow EL signal at 350 mA with comparison to the spectrum at zero current.

As a reference, we also performed a direct temperature-dependent Raman measurement by placing the LED in a heating chamber (TS1500, Linkam) from room temperature to 120 °C, with the results shown in Fig. 3(d). We realize that the amount of Raman peak shift of the E_2^H mode is less than 1 cm⁻¹ between 40 °C and 100 °C, which could lead to a large uncertainty if one uses this dependence to extract the temperature change, not to mention the complication due to the stress relaxation [18]. For comparison, we also use the forward-voltage method to measure the temperature difference between the LED and heat sink by placing the LED in a heating chamber (HCP621GP, INSTEK Inc.).

The relative intensity ratio of Stokes and anti-Stokes Raman scattering is known to be sensitive to the temperature and is often used as the temperature metric [23,24]

$$\frac{I^{AS}}{I^S} = M \left(\frac{\nu_o + \nu_i}{\nu_o - \nu_i} \right)^4 \exp \left(-\frac{h\nu_i}{kT} \right), \quad (1)$$

where I^{AS} and I^S are the intensity of anti-Stokes and Stokes Raman peaks, ν_o is the frequency of the incident light, ν_i is the Raman shift, k is the Boltzmann constant, and h is the Plank constant. M is a correction factor that depends on multiple effects, such as the spectral dispersion of the

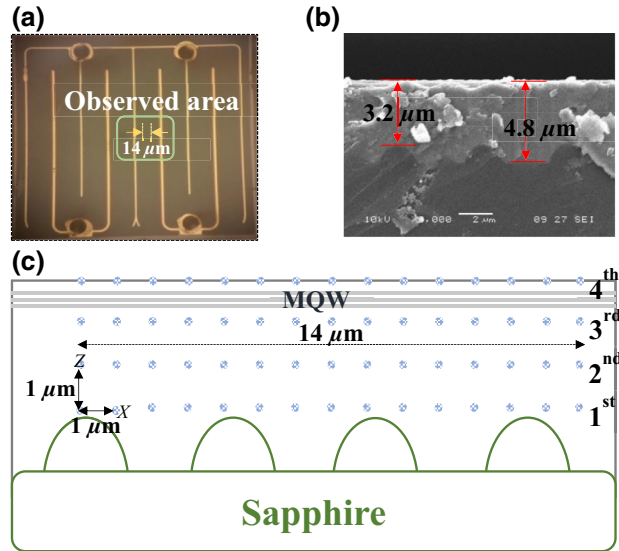


FIG. 4. Top and cross-sectional images of the LED, and temperature probing points on the device cross section. (a) Top view of optical microscope image, (b) cross-sectional SEM image, and (c) cross-sectional schematic drawing showing the measured locations (blue dots) at four different depths.

spectroscopy system and material. In order to determine M , multiple Raman spectra are measured with the GaN LED placed on a hot plate maintained at constant temperatures of 24 °C and 85 °C under a no-biased condition in order to avoid temperature fluctuation. Applying Eq. (1) to the 24 °C data yielded $M = 0.854 \pm 0.0016$, with an uncertainty of ± 2.07 °C; and to the 85 °C $M = 0.853 \pm 0.0011$, with an uncertainty of ± 2.01 °C. The results of ten repeated measurements at 24 °C from a single location are plotted in the inset of Fig. 3(c), showing the excellent repeatability and reliability of the method. Note that, in the temperature range of interest to this work, M remains nearly constant. For a general case, one can use an explicitly measured $M(T)$ function in Eq. (1).

Figures 4(a) and 4(b) show a top-view optical microscope image of the LED with interdigitated n and p electrodes and a cross-sectional scanning electron microscope (SEM) image, respectively. The thickness of the GaN film is found to be approximately 4.8 μm from the flat portion of the sapphire substrate and approximately 3.2 μm from the top of the pillars of the patterned sapphire structure, as shown in the SEM image Fig. 4(b). For the purpose of demonstrating the feasibility of the methodology, we probed the device temperature profiles in one horizontal plane within one small volume at the central region between a pair of n and p electrodes as indicated in Fig. 4(a). The vertical ($x, y = 0, z$) plane is illustrated in Fig. 4(c), which is 14 μm in width and 3 μm in height, covering a cross-sectional area from the bottom to the top of the GaN film. The lateral and vertical distances of the

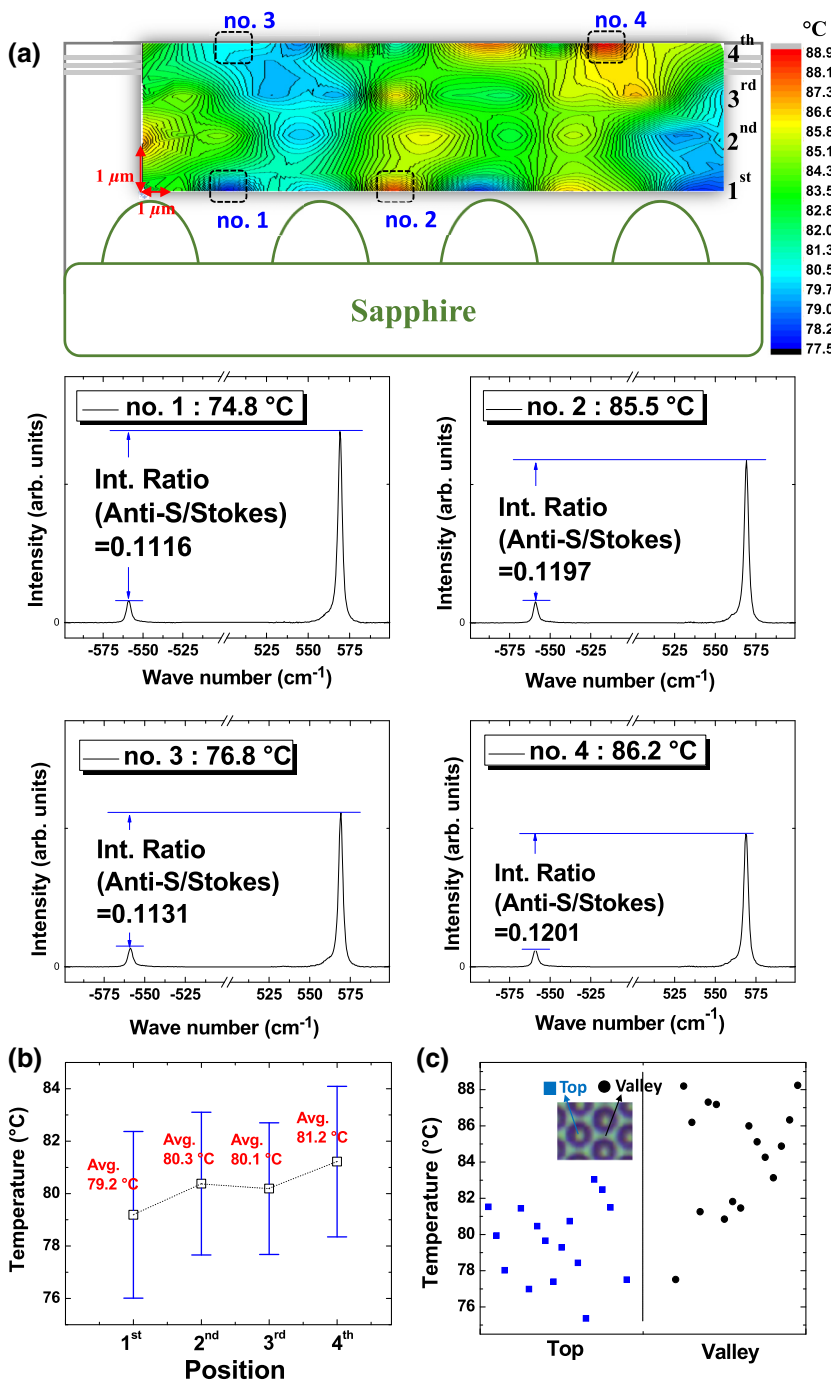


FIG. 5. 3D temperature profile sampling results. (a) Cross-sectional temperature contours calculated from the intensity ratio of Stokes and anti-Stokes Raman scattering and Raman spectra of a few extreme points (no. 1 to no. 4) below. (b) Average temperatures at different depths. (c) Scattered plots of temperatures at two types of sites (“top” and “valley”) at first depth.

data points are all approximately 1 μm, with a total of 60 locations where Raman spectra are measured. The horizontal ($x, y, z = 0$) plane is at the bottom of the vertical plane aligned with the top sites of the patterned sapphire structure.

Figure 5(a) depicts the temperature contour in the x - z cross section calculated with Eq. (1). The overall temperature profile looks like a columnar shape along the vertical direction. Assuming the LED junction temperature is the same as the top surface temperature, we find that at 350 mA the average temperature difference is only approximately

2 °C between the top and bottom of the GaN epilayer, as shown in Fig. 5(b). However, we note that the magnitude of temperature fluctuation within the same depth can be significantly larger than the overall laterally averaged variation in the depth direction, because for various reasons the device simply does not have an axial symmetry to justify using a one-dimensional (1D) model. Within the cross section, the maximum temperature of 86.2 °C (location no. 4) is measured at the top surface and a minimum temperature of 74.8 °C (no. 1) is measured at the bottom surface close to the sapphire substrate. Raman spectra of a

few extreme points (no. 1 to no. 4) are included in Fig. 5(a). Moreover, we find that, despite some fluctuation, on average the GaN temperature near the top of the patterned sapphire pillars is lower than that of the region between the top sites at the same height. Figure 5(c) plots the temperatures from 32 locations for each of the two types of sites and the averaged difference is approximately 5.7 °C. The averaged difference and the fluctuation within the nominally equivalent sites can be qualitatively understood in terms of the specific lateral growth mechanism [25]. It is possible that the GaN material near the pillar top is less defective on average and, thus, typically has higher thermal conductivity compared to the region right above the flat sapphire, although the GaN/sapphire contact at the pillar top can vary from one site to another. We note that only the average temperature difference between the heat sink and the junction was measured previously [8–11]. Here we are able to probe the full 3D distribution to assess the thermal management needs between different materials, such as the interface of the epilayer and substrate, and different regions of the same material, such as at different distances from the electrodes.

Based on the average temperatures of the third and fourth depths in Fig. 5(b), the average junction temperature can be estimated to be between 80.1 °C and 81.2 °C at 350 mA. The forward-voltage method [8] is typically used to obtain an average junction temperature. In order to make a direct comparison of the two methods, the forward-voltage method is applied to the same GaN LED. The forward voltage declines linearly from 3.23 V at room temperature to 3.17 V as the ambient temperature increases from room temperature to 85 °C (not shown here). When under a 350-mA current injection for 18 s, the forward voltage reaches 3.18 V, corresponding to 82.5 °C. This result is similar to the average temperature acquired from the Stokes and anti-Stokes Raman scattering in this study.

Finally, we note that the 3D temperature variations measured using the anti-Stocks and Stokes Raman ratio are more accurate and reliable than those obtained using the Raman frequency shift. For instance, the temperature distribution measured using the Raman frequency shift would result in significantly lower temperatures and much larger average temperature differences, 66.0 °C for the top sites and 80.6 °C for the valley sites, because the strain relaxation with increasing temperature is likely rather significant near the GaN/sapphire interface due to the very large lattice mismatch and the coefficient of thermal expansion.

IV. CONCLUSION

In conclusion, we develop a technique that can offer 3D temperature profiling with approximately 1- μ m spatial

resolution for semiconductor devices where major self-heating is expected under realistic operation conditions, such as high-power LEDs, lasers, concentrated photovoltaics (PV), and power electronics devices, and demonstrate the technique with an $(In_xGa_{1-x})N/GaN$ LED. We show that using the Stokes and anti-Stokes Raman scattering ratio can yield more reliable and accurate temperature values without the complication of strain relaxation than if one uses the Raman frequency shift. In the specific device examined, despite the fact that on average the surface temperature of GaN LEDs is only slightly higher (by approximately 2.0 °C) than the bottom part of the GaN film, the magnitude of the lateral temperature variation can be significantly larger than this averaged vertical change. Also, the temperature at the pillar-top sites of the patterned sapphire structure is lower by approximately 5.7 °C on average than that of the valley sites. These previously unnoticed 3D temperature variations indicate the necessity of a 3D probing technique to properly analyze the device performance. Although current implementation is to mimic the cw operation, it can be modified to mimic pulse operation as well. This technique may have broad applications for Raman spectroscopy-based 3D thermometry that can offer both high accuracy and spatial resolution.

ACKNOWLEDGMENTS

The work at UNCC was supported by ARO/Electronics (Grant No. W911NF-16-1-0263) and at IOS by the National Key Research and Development Program of China (Grant No. 2016YFB0400102) and Guangzhou Science & Technology Project of Guangdong Province, China (Grants No. 201704030106 and No. 2016201604030035).

- [1] S. Nakamura, M. Senoh, N. Iwasa, and S.-I. Nagahama, High-brightness InGaN blue, green and yellow light-emitting diodes with quantum well structures, *Jpn. J. Appl. Phys.* **34**, L797 (1995).
- [2] J. Cho, E. F. Schubert, and J. K. Kim, Efficiency droop in light-emitting diodes: Challenges and countermeasures, *Laser Photonics Rev.* **7**, 408 (2013).
- [3] B. J. Baliga, Gallium nitride devices for power electronic applications, *Semicond. Sci. Technol.* **28**, 074011 (2013).
- [4] E. A. Jones, F. (Fred) Wang, and D. Costinett, Review of commercial GaN power devices and GaN-based converter design challenges, *IEEE J. Emerg. Sel. Top. Power Electron.* **4**, 707 (2016).
- [5] D. S. Meynard, Q. Shan, J. Cho, E. F. Schubert, S.-H. Han, M.-H. Kim, C. Sone, S. J. Oh, and J. K. Kim, Temperature dependent efficiency droop in GaInN light-emitting diodes with different current densities, *Appl. Phys. Lett.* **100**, 081106 (2012).
- [6] X. Guo and E. F. Schubert, Current crowding in GaN/InGaN light emitting diodes on insulating substrates, *J. Appl. Phys.* **90**, 4191 (2001).
- [7] M. Kuball, J. M. Hayes, M. J. Uren, T. Martin, J. C. H. Birbeck, R. S. Balmer, and B. T. Hughes, Measurement

- of temperature in active high-power AlGaN/GaN HFETs using Raman spectroscopy, *IEEE Electron. Device Lett.* **23**, 7 (2002).
- [8] Y. Xi and E. F. Schubert, Junction-temperature measurement in GaN ultraviolet light-emitting diodes using diode forward voltage method, *Appl. Phys. Lett.* **85**, 2163 (2004).
- [9] S. Murata and H. Nakada, Adding a heat bypass improves the thermal characteristics of a 50 μm spaced 8-beam laser diode array, *J. Appl. Phys.* **72**, 2514 (1992).
- [10] J. Cho, C. Sone, Y. Park, and E. Yoon, Measuring the junction temperature of III-nitride light emitting diodes using electro-luminescence shift, *Phys. Status Solidi (a)* **202**, 1869 (2005).
- [11] D. C. Hall, L. Goldberg, and D. Mehuys, Technique for lateral temperature profiling in optoelectronic devices using a photoluminescence microprobe, *Appl. Phys. Lett.* **61**, 384 (1992).
- [12] J. Senawiratne, A. Chatterjee, T. Detchprohm, W. Zhao, Y. Li, M. Zhu, Y. Xia, X. Li, J. Plawsky, and C. Wetzel, Junction temperature, spectral shift, and efficiency in GaInN-based blue and green light emitting diodes, *Thin Solid Films* **518**, 1732 (2010).
- [13] J. Senawiratne, Y. Li, M. Zhu, Y. Xia, W. Zhao, T. Detchprohm, A. Chatterjee, J. L. Plawsky, and C. Wetzel, Junction temperature measurements and thermal modeling of GaInN/GaN quantum well light-emitting diodes, *J. Electron. Mater.* **37**, 607 (2008).
- [14] J. Zhang, T. Shih, Y. Lu, H. Merlitz, R. R.-G. Chang, and Z. Chen, Non-synchronization of lattice and carrier temperatures in light-emitting diodes, *Sci. Rep.* **6**, 19539 (2016).
- [15] K. S. Chang, S. C. Yang, J.-Y. Kim, M. H. Kook, S. Y. Ryu, H. Y. Choi, and G. H. Kim, Precise temperature mapping of GaN-based LEDs by quantitative infrared micro-thermography, *Sensors* **12**, 4648 (2012).
- [16] W. Grieshaber, E. F. Schubert, I. D. Goepfert, R. F. Karlicek, Jr., M. J. Schurman, and C. Tran, Competition between band gap and yellow luminescence in GaN and its relevance for optoelectronic devices, *J. Appl. Phys.* **80**, 4615 (1996).
- [17] T. Beechem, A. Christensen, S. Graham, and D. Green, Micro-Raman thermometry in the presence of complex stresses in GaN devices, *J. Appl. Phys.* **103**, 124501 (2008).
- [18] J. Zheng, S. Li, C. Chou, W. Lin, F. Xun, F. Guo, T. Zheng, S. Li, and J. Kang, Direct observation of the biaxial stress effect on efficiency droop in GaN-based light-emitting diode under electrical injection, *Sci. Rep.* **5**, 17227 (2015).
- [19] J. Xie, X. Ni, Q. Fan, R. Shimada, Ü. Özgür, and H. Morkoç, On the efficiency droop in InGaN multiple quantum well blue light emitting diodes and its reduction with p-doped quantum well barriers, *Appl. Phys. Lett.* **93**, 121107 (2008).
- [20] Z. Li, T. Marron, H. Naik, W. Huang, and T. P. Chow, in *Proceedings of the 22nd International Symposium on Power Semiconductor Devices & IC's (ISPSD), NM-P4*, Hiroshima, Japan (2010).
- [21] Y. Lin, Y.-L. Gao, Y.-J. Lu, L.-H. Zhu, Y. Zhang, and Z. Chen, Study of temperature sensitive optical parameters and junction temperature determination of light-emitting diodes, *Appl. Phys. Lett.* **100**, 202108 (2012).
- [22] S. P. Kearney, L. M. Phinney, and M. S. Baker, Spatially resolved temperature mapping of electrothermal actuators by surface Raman scattering, *J. Microelectromech. Syst.* **15**, 314 (2006).
- [23] H. Tsuji, A. Oda, J. Kido, T. Sugiyama, and Y. Furukawa, Temperature measurements of organic light-emitting diodes by Stokes and Anti-Stokes Raman scattering, *Jpn. J. Appl. Phys.* **47**, 2171 (2008).
- [24] H. W. Lo and A. Compaan, Raman Measurement of Lattice Temperature During Pulsed Laser Heating of Silicon, *Phys. Rev. Lett.* **44**, 1604 (1980).
- [25] L. Meng, W. Guohong, L. Hongjian, L. Zhicong, Y. Ran, W. Bing, L. Panpan, L. Jing, Y. Xiaoyan, W. Junxi, and L. Jinmin, Low threading dislocation density in GaN films grown on patterned sapphire substrates, *J. Semicond.* **33**, 113002 (2012).